RSC Advances

ROYAL SOCIETY OF CHEMISTRY

www.rsc.org/advances

Investigation of the continuous flow sorption of heavy metals through biomass-packed column: Revisiting Thomas design model for correlation of binary component systems

Felycia E. Soetaredjo, Alfin Kurniawan, L.K. Ong, Dimas R. Widagdyo, Suryadi Ismadji

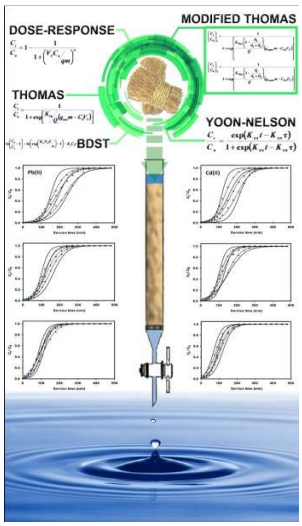

A new column model based on the semi-empirical modification of the original Thomas model was proposed in this study for the correlation of the breakthrough curves for adsorption of bicomponent heavy metals onto biomass-packed column.

Investigation of the continuous flow sorption of heavy metals through biomass-packed column: Revisiting Thomas design model for correlation of binary component systems

Felycia E. Soetaredjo*, Alfin Kurniawan, L.K. Ong, Dimas R. Widagdyo, Suryadi Ismadji

Department of Chemical Engineering, Widya Mandala Surabaya Catholic University, Kalijudan 37, Surabaya 60114, East Java, Indonesia

* Corresponding author: Felycia E. Soetaredjo, e-mail address: felyciae@yahoo.com, Tel.: +62 31 389 1264, Fax: +62 31 389 1267

Abstract

Remediation of aquatic environments that are polluted by toxic heavy metals has become a focus of interests for most chemical and environmental engineers throughout the world. In this study, rice straw was utilized as a low cost agricultural waste material to remove Cd(II) and Pb(II) ions from single and binary solutions. The isothermal biosorption experiments at 303.15 K were conducted in a column mode at various flow rates and bed heights. The breakthrough curves for single metal systems were fitted with the Thomas, Yoon-Nelson, bed-depth-service-time (BDST) and dose-response models. A new semi-empirical model based on the classical Thomas equation was developed for simulation of the breakthrough curves for binary metal systems. The modified Thomas model, incorporated with the sorption-inhibiting coefficients that account for competitive sorption behavior, was able to represent the breakthrough data very well. The exhausted biosorbent bed could be easily regenerated by an acid elution method using 0.05 mol L^{-1} HCl solution and reused for five consecutive sorption-regeneration cycles without considerable loss in the adsorption capacity. The utilized biosorbent also showed a promising application for economical packed bed treatment of real electroplating wastewater containing Cd(II) and Pb(II) ions.

Keywords: Rice straw; Heavy metal; Biosorption; Breakthrough analysis; Binary metal system; Modified Thomas model; Waste management

1. Introduction

With rapidly growing of urban population and industrialization, the reserves and quality of surface waters are worsening due to excessive input of pollutants into the water bodies. Among various types of water pollutants, heavy metals are the most life-threatening, attributable to their toxicity, carcinogenicity, insusceptible to biological degradation and long-term accumulation in the food chains.[1] Cadmium and lead are two heavy metals that have many desirable properties in a variety of industrial workplaces such as batteries, ammunition, electronic goods, metal finishing, weighting and shielding applications. According to the priority list of hazardous substances issued by the U.S. Agency for Toxic Substances and Disease Registry (ATSDR), lead and cadmium ranks second and seventh respectively in terms of their frequency of occurrence, toxicity level and potential for human exposure.[2] Therefore, the removal of these heavy metals is an essential effort, not only considered as environmental awareness but also for the protection of water resources.

Over the last decade, adsorption is likely to become the method of choice for purification of water and wastewater. The key advantages of adsorption method include high efficiency, cost-effective, wide adaptability, environmentally acceptable and capable of generating high quality effluents. The success of adsorption process strongly relies on the selection of adsorbent material and design of the separation unit. For the adsorption of heavy metals, living or dead microbial and seaweed biomass, cellular products, activated carbons, sewage sludges, clays/clay minerals, hybrid materials, ordered mesoporous silica, etc. have been tested.[3-12] Among them, living or dead lignocellulosic biomass consisting of natural polymeric materials are the promising candidate alternative to commercial adsorbents for purification of metal-bearing effluents. These natural polymeric materials (i.e., lignin, cellulose and hemicellulose) contain hydroxyl, carboxyl, phosphate and amino functional

groups, which all possess specific affinity to bind the heavy metals.[13-15] To that end, leftover of rice straw (about 40 million tons per annum are found in Indonesia) is highlighted as a cheap and potential biomass for heavy metals detoxification from aqueous solution in the present study.

In practical applications, adsorption operation is usually performed in a packed bed system where the effluent stream is passed a column packed with a given quantity of suitable adsorbent. The reliable design of packed bed adsorber requires the construction of satisfactory modeling framework centered on establishing the shape of the breakthrough curve.[16] The characteristic shape of the breakthrough curve of an adsorption system strongly depends on the design data such as flow rate, initial solute concentration and the adsorber dimension. In recent years, an increasing number of publications dealing with heavy metals adsorption in a packed bed operation and the breakthrough modeling can be found in literatures.[17-21] However, these studies pertaining to the single-solute adsorption are less describing real situation in the industrial wastewater treatment.

In real wastewater treatment, two or more heavy metal species may coexist within the liquid system. Although a large number of studies have sought to establish different mathematical models for simulating the breakthrough curves for binary or multicomponent systems, there is still a big challenge to construct a simple yet reliable model with high accuracy and also computationally efficient. The building block of most breakthrough models for heavy metal sorption is based on the rate-controlling mechanisms and typical examples are film diffusion, surface diffusion, pore diffusion and their combinations.[22-24] Most, if not all, of these mass transfer-based models have found limited success due to complexity of the modeling, which often requires advanced computer resources for solving the model. On the other hand, a semi-

empirical modification on the well-established column model can be considered as a more effective approach to construct the breakthrough curves which are closer matched to experimental data. In line with this, the present study aims to propose a new column model based on the classical Thomas model for simulation of the breakthrough curves of heavy metals (i.e., Cd(II) and Pb(II)) sorption from binary mixtures. The effects of the bed height and flow rate on the breakthrough characteristics for single and binary metal systems are discussed in detail. The practical application of rice straw in handling real electroplating wastewater containing multiple metal ions is also evaluated with respect to the adsorption performance and cycling efficiency along with possibility to transform the waste biosorbent into value-added products.

2. Experimental

2.1. Chemicals

Cadmium nitrate tetrahydrate (98%) and lead nitrate (99%) were purchased as analytical grade from Sigma-Aldrich Co., Singapore and used as-supplied. Deionized water was used throughout the experiments.

2.2. Preparation of biosorbent

Rice straw was collected from a rice field located at Blitar district, East Java. After the collection, the biomass was cut into a size of 1×1 cm and boiled with deionized water (solid/water ratio of 1:10, three stages for 3 h during each stage) to remove color materials and water-soluble compounds. The solid was then separated by vacuum filtration, washed and dried in a forced convection oven at 80 °C for 48 h. The dried biomass was crushed using an IKA-Labortechnick grinder and sieved pass through a US standard test sieve No. 50/60 (250-297 μm). The final product was kept in the airtight plastic bags for further experiments.

2.3. Packed-bed biosorption experiments

Cadmium and lead solutions were prepared by dissolving a fixed amount of nitrate salt of metal reagents into 1 L deionized water to give an initial concentration of 0.01 mmol L^{-1}. Laboratory-scale experiments were conducted in a glass column (3 cm i.d., length of 40 cm) supported with 0.2 cm layer of Por.2 grade sintered discs (United Scientific Industries) installed at the top and bottom of the column to ensure a closely packed arrangement and prevent any loss of biosorbent. A programmable Masterflex™ L/S peristaltic pump (Cole-Parmer Instrument Co.) was used to maintain constant flow rate. The experimental setup is depicted in the supplementary information Figure S1. A given quantity of biosorbent was tightly packed into the column to give a bed height of 10 cm, 15 cm and 20 cm. Precautions were taken to avoid the flow channeling and entrapping of air pockets within the packed bed by soaking the column in deionized water for 2 h before starting biosorption experiments. Then, $Cd(NO_3)_2$, $Pb(NO_3)_2$, or an equimolar mixture of $Cd(NO_3)_2$ and $Pb(NO_3)_2$ was continuously pumped to the top of the column (downflow mode) at a prescribed flow rate (i.e., 10, 20 and 30 ml min^{-1}). Solution of 0.1 N HCl was used to adjust the pH of metal effluents to a value between 5.5 and 6. The column experiments were conducted at room temperature for 8 h. Preliminary investigation showed that 8 h was the bed exhaustion time (t_e, the time at which solute concentration in the outlet stream reached 95% of its initial concentration). Effluent samples from the exit of the column were collected periodically and analyzed for the residual ion concentration. In the first period of the experiments (2 h), aliquots of 5 ml were collected every 15 min and then every half an hour in the remaining duration. Duplicate runs were taken and data are given as mean values of two replications.

2.4. Analysis of the residual concentrations of metal ions

The residual concentrations of Cd(II) and Pb(II) ions in the outlet stream were analyzed on a Shimadzu AA-6200 atomic absorption flame emission spectrophotometer in an air-acetylene flame. The calibration curves of each metal were constructed by diluting standard solutions of $Cd(NO_3)_2$ and $Pb(NO_3)_2$ (Fisher Scientific) to obtain working solutions with varying concentrations (0.001 to 0.01 mmol L^{-1}). The maximum absorbance was measured at a detection wavelength of 217.0 nm for Pb(II) and 228.8 nm for Cd(II).

2.5. Characterizations of biosorbent

The surface topography was visualized on a JEOL JSM-6300F field emission SEM at an accelerating voltage of 20 kV. An energy dispersive X-ray (EDX) detection system was connected to SEM for elemental analysis. N_2 adsorption isotherms were measured at 77 K using a Micromeritics ASAP 2010 automated sorptometer. The specific surface area was determined by standard BET method applied to adsorption branch in the relative pressure ($p/p°$) range of 0.05-0.30. Total pore volume (V_T) was estimated from the amount of N_2 adsorbed at a relative pressure of 0.99. The analysis of metal contents was conducted on a PANalytical MiniPal QC energy dispersive X-ray fluorescence (EDXRF) spectrometer. The surface functional groups were identified by infrared spectroscopy on a Shimadzu FTIR 8400S spectrophotometer.

2.6. Calculations

The amounts of metal ions adsorbed onto packed biosorbent, also defined as the dynamic uptake capacity (mmol g^{-1}) were calculated by Eq. (1):

$$q_{\text{bed}} = M_r / m \qquad (1)$$

where m is the mass of packed biosorbent (g) and M_r represents the difference between influent metal load (mmol) and the escaping one from the column (mmol). The parameter M_r can be determined by the following equation[25]:

$$M_r = V_e C_0 - \sum \frac{(V_{n+1} - V_n)(C_{n+1} - C_n)}{2} \quad (2)$$

where V_e is the throughput volume at column exhaustion (L), C_0 is the influent metal concentration (mmol L^{-1}), V_n is the throughput volume at nth reading (L), V_{n+1} is the throughput volume at (n+1)th reading (L), C_n is the outlet metal concentration at nth reading (mmol L^{-1}) and C_{n+1} is the outlet metal concentration at (n+1)th reading (mmol L^{-1}). The quantity of metal ions in the adsorbed phase at 1% breakthrough, q_b (mmol g^{-1}), can be determined from the following relation[26]:

$$q_b = \frac{Q \times t_{1\%} \times C_0}{1000 \times m} \quad (3)$$

where $t_{1\%}$ is the column service time (min) when the outlet solute concentration is equivalent to 1% of the inlet one, Q is the flow rate (ml min^{-1}) and m is the mass of packed biosorbent (g).

3. Results and discussion

3.1. Characteristics of biosorbent

The electron micrographs in the supplementary information Figures S2(a)-(c) show a rod-like structure, smooth and uniform surface of native rice straw. The EDX spectrum shown in Figure S2(d) confirms that silica and alkali and alkaline earth metals (i.e., Na, K and Ca) are the elemental constituents of native rice straw. The presence of cadmium and lead metals is detected in the EDX spectrum of metal-loaded rice straw (Fig. S2(e)), verifying that these metals are adsorbed on the surface of biosorbent. SEM images also reveal that there are no significant structural changes between native and metal-loaded rice straw. The BET specific

surface area of native rice straw was fairly low (39.6 m^2 g^{-1}) with total pore volume of 0.012 cm^3 g^{-1}, supporting SEM information that the biosorbent is a non-porous material.

FTIR transmittance spectra (figure not shown here) display several representative bands of native rice straw: stretching of H-bonded OH groups at 3418 cm^{-1}, symmetrical stretching of sp^3 C–H in CH_2 group near 2850 cm^{-1}, stretching of C=O assigned to carboxylic acids or aliphatic esters in lignin or hemicellulose at 1758 cm^{-1}, stretching of C=C in the aromatic rings of bound lignin at 1520 cm^{-1}, symmetrical sp^3 C–H bending at 1361 cm^{-1}, stretching of C–O corresponds to glycosidic linkages in cellulose and hemicellulose near 1100 cm^{-1}, out-of-plane sp^2 C–H bending at 675 cm^{-1} and Si–O–Si stretching in silica at 524 cm^{-1}. The binding of Cd(II) and Pb(II) on the surface of biosorbent was evidenced by the absorption bands within 510-450 cm^{-1} that possibly arise from stretching vibration of M–O bonding where M refers to divalent Cd(II) or Pb(II) cations. Specifically, the coordination modes of metal-carboxylate complexes can be categorized into unidentate coordination, bidentate chelating coordination or bidentate bridging coordination.[27] By taking into account the spectral information of $\Delta\nu(COO^-)_{complex}$ and the possibility of interaction between divalent metal atom and the second carboxylate oxygen of the COO^- moiety present in cellulose and hemicellulose structures, it can be suggested that Cd(II)-carboxylate or Pb(II)-carboxylate complexes coordinate in the bidentate bridging form. In this case, the bidentate carboxylate-binding mode is preferred over the monodentate mode in order to minimize the steric repulsion between the incoming metal ions and the ligand moiety. Furthermore, the clear shifts in the position of stretching peaks of hydroxyl and carboxylic groups near 3400 and 1750 cm^{-1} to lower wavenumbers show chemical interactions involving metal species and these surface functional groups in the biosorption process.

3.2. Breakthrough analysis

3.2.1. Effects of bed height

The effects of biosorbent dosage on the dynamic uptake capacity were systematically examined by varying bed heights at a constant flow rate and initial metal concentration of 0.01 mmol L^{-1}. In this study, the performance of packed bed was determined over relative concentrations (C_t/C_0) from 0.01 (1% breakthrough) to 0.95 (95% breakthrough) by considering safe water quality standard regulated by local government. In Fig. 1, it can be seen that the gradient of the breakthrough curves becomes less sharp with increasing bed height, representing a greater extent of bed uptake capacity. The mass transfer zone (MTZ) (i.e., the active part of the packed bed where adsorption actually operates) in the Cd(II)-loaded column is 7.67, 10.47 and 11.96 cm for 10, 15 and 20-cm bed height respectively. Longer time to reach the break point is also accomplished with beds of an increased height. The dynamic uptake capacity at 1% breakthrough for a 15-cm packing height was 6.20×10^{-4} mmol g^{-1} (0.070 mg g^{-1}) for cadmium and 6.72×10^{-4} mmol g^{-1} (0.139 mg g^{-1}) for lead and these values are increased to 6.74×10^{-4} mmol g^{-1} (0.076 mg g^{-1}) and 7.30×10^{-4} mmol g^{-1} (0.151 mg g^{-1}) respectively for a 20-cm bed height by feeding the effluent at 10 ml min^{-1}. This indicates that higher bed height provides longer distance of MTZ for the metal effluent to pass by before reaching the exit, thus allowing for a delayed breakthrough and an increase in the throughput volume of solution treated and ultimately extending the lifetime of the bed. With regard to bed exhaustion time, the beds with smaller heights are saturated in a shorter period of time due to less number of the superficial areas of the adsorbent and consequently the active sites available for sorption.

3.2.2. Effects of solution flow rate

The breakthrough curves for single biosorption of Cd(II) and Pb(II) ions at various flow rates are shown in Figure 1. The increased steepness of the breakthrough curves was noticed at higher flow rate, demonstrating an early breakthrough time and bed exhaustion time. For a 20-cm bed height, the breakthrough time and exhaustion time was shortened from 171 to 73 min and from 395 to 300 min as the solution flow rate increases from 10 to 20 ml min^{-1} for Pb(II) sorption. The results can be explained by considering the limited contact time between metal effluent and biosorbent bed and also the diffusion limitation of metal ions from liquid phase to solid phase at higher flow rate thus reducing the volume of solution being treated and consequently a decrease in the dynamic uptake capacity. Furthermore, lower adsorption capacity at 1% breakthrough was obtained with higher flow rate. For example, the 20-cm breakthrough capacity of Cd(II) was decreased from 6.74×10^{-4} mmol g^{-1} (0.076 mg g^{-1}) to 5.72×10^{-4} mmol g^{-1} (0.064 mg g^{-1}) by doubling the flow rate from 10 to 20 ml min^{-1} and further decrease in the breakthrough capacity to 4.48×10^{-4} mmol g^{-1} (0.050 mg g^{-1}) was noted with increasing flow rate to 30 ml min^{-1}.

3.3. Breakthrough modeling for biosorption of single metals

The design and optimization of the breakthrough curve for a full-scale column adsorption system requires a simple modeling approach that can provide accurate scale-up column data. In this study, Thomas, Yoon-Nelson, bed-depth-service-time (BDST) and dose-response empirical models were applied to analyze the breakthrough curves for single metal systems. The Thomas model is one of the most celebrated models used for describing the column performance and the breakthrough curve, which is derived based on the Langmuir adsorption-desorption isotherms for the equilibrium and the second-order reversible reaction kinetics for the rate driving force without external and intraparticle diffusion limitations.[28] Thomas model has the following form:

$$\frac{C_t}{C_0} = \frac{1}{1 + \exp\left[K_{\mathrm{Th}} / Q \left(q_{\max} m - C_0 V_T \right) \right]} \quad (4)$$

where K_{Th} is the Thomas rate constant (mL mmol^{-1} min^{-1}), $q_{\max}$ is the intrinsic property of the adsorbent that represents the maximum solid-phase concentration of solute (mmol g^{-1}), m is the mass of adsorbent (g), C_0 is the inlet concentration of solute (mmol L^{-1}), C_t is the exit concentration of solute at time t (mmol L^{-1}), Q is the solution flow rate (ml min^{-1}) and V_T is the cumulative throughput volume of treated solution (L). The determination of Thomas parameters (i.e., K_{Th} and $q_{\max}$) was conducted by plotting ln (C_0/C_t – 1) versus t to give a straight line with slope and intercept of $K_{\mathrm{Th}} \bullet C_0$ and ($K_{\mathrm{Th}} \bullet q_{\max} \bullet m$)/$Q$, respectively.

The second model applied for correlating the breakthrough curve was Yoon-Nelson model. This model was developed by supposing that the rate of decrease in the probability of adsorption for each solute is proportional to the probability of its sorption and the breakthrough on the adsorbent.[29] The original and linearized forms of Yoon-Nelson model for single component adsorption are expressed as follows:

$$\frac{C_t}{C_0} = \frac{\exp\left(K_{\mathrm{YN}} t - K_{\mathrm{YN}} \tau\right)}{1 + \exp\left(K_{\mathrm{YN}} t - K_{\mathrm{YN}} \tau\right)} \quad (5)$$

$$\ln \frac{C_t}{C_0 - C_t} = K_{\mathrm{YN}} t - K_{\mathrm{YN}} \tau \quad (6)$$

Here, τ is the theoretical time required to achieve 50% adsorbate breakthrough in min and K_{YN} is the Yoon-Nelson rate constant in min^{-1}. The third model used for the breakthrough curve analysis was BDST model. The underlying assumption of the BDST model is that the adsorption rate is proportional to both the unused capacity of the adsorbent and the remaining concentration of solute in the liquid phase by neglecting axial dispersion factor. The BDST model is considered to be a simple yet reliable model based on physically measuring the

adsorption capacity of the bed at different breakthrough values. The classical BDST model has the following expression[30]:

$$\ln\left(\frac{C_0}{C_b}-1\right)=\ln\left(\exp\left(K_a N_0 Z/u\right)-1\right)-K_a C_0 t \qquad (7)$$

where C_b is the desirable breakthrough concentration (mmol L^{-1}), Z is the bed height (cm), N_0 is the volumetric sorption capacity of the bed (mmol L^{-1}), K_a is the adsorption rate constant (L $mmol^{-1}$ min^{-1}) and u is the linear velocity obtained by dividing solution flow rate with cross-sectional area of the bed (cm min^{-1}). Eq. (7) was further modified by Hutchins[31] in order to estimate the required bed height for a given service time at breakthrough point:

$$t_b=\frac{N_0}{C_0 u}Z-\frac{1}{K_a C_0}\ln\left(\frac{C_0}{C_b}-1\right) \text{ when } \exp\left(K_a N_0 Z/u\right) >> 1 \qquad (8)$$

Solving Eq. (8) for Z by substituting $t_b = 0$ gives:

$$Z_0=\frac{u}{N_0 K_a}\ln\left(\frac{C_0}{C_b}-1\right) \qquad (9)$$

where Z_0 is the minimum theoretical height required to give an exit concentration of C_b at zero time. Often, Z_0 is referred to as the critical bed height and clearly is equal to mass transfer zone length (MTZL). The dose-response model, firstly proposed by Viraraghavan and his group[32] is an empirical model to describe biosorption of heavy metals in column operation. Generally, this model is capable to describe the kinetics of metal removal by the adsorption column more adequately compared to the Bohart-Adams or Thomas models, especially at lower and higher time periods of the breakthrough curve. The mathematical expression of the dose-response model is presented below:

$$\frac{C_t}{C_0}=b_0-\frac{b_0}{1+\left(V_T/b_1\right)^d} \qquad (10)$$

where parameter b_0 is the expected response when saturation is reached and it is equal to unity as the time or throughput volume tends to infinity. The parameter b_1 indicates the throughput volume at which half of the maximum response occurs and m is a constant of the model. The dose-response model can be expressed in another formula by setting $b_0 = 1$:

$$\frac{C_t}{C_0} = 1 - \frac{1}{1 + \left(V_T C_0 / qm \right)^d} \text{ with } b_1 = qm / C_0 \tag{11}$$

The regression analysis of all column models against experimental breakthrough data was performed using Systat SigmaPlot 12.3.1 software and the correlation model parameters obtained were used to construct the predicted breakthrough curves shown in Fig. 2. The accuracy of prediction of the models was further evaluated by computing the root mean square error (RMSE), defined as follows:

$$\text{RMSE} = \sqrt{\frac{1}{N} \sum_{i=1}^{N} \left(y_{i,\text{exp}} - y_{i,\text{cal}} \right)^2} \tag{12}$$

where N is the number of experimental data, $y_{i,\text{exp}}$ and $y_{i,\text{cal}}$ are the values obtained from experiments and predictions, respectively.

As shown in Figure 1, it can be seen a very good agreement between the experimental and predicted column data by the Thomas, Yoon-Nelson and dose-response models. The coefficient of determination (R^2) found for the three models are mostly greater than 0.94. The column correlation coefficients associated to each model are listed in Tables 2 and 3. The values of the rate constants for Thomas (K_{Th}) and Yoon-Nelson (K_{YN}) models decrease with increase in bed height and decrease in flow rate. The relation between rate constant and bed height can be justified on the basis of the rate at which the MTZ traveled through the bed decreased with bed height due to increasing number of service area to treat the effluent. Higher rate constant suggests that a shorter bed would be sufficient to avoid breakthrough.[33]

The maximum bed adsorption capacity obtained from the Thomas model prediction ranged between 0.92×10^{-3} and 1.79×10^{-3} mmol g^{-1} within the experimental conditions. However, the prediction overestimated the q_{bed} values obtained from Eq. (1) by about 10-21%. This conspicuously difference was also encountered in several column studies.[34-36] The increasing adsorption rate constant with flow rate might be attributed to a decrease in the fluid-film mass transfer resistance so that solute molecules could diffuse more easily from liquid phase to solid phase. The correlation of column data by Yoon-Nelson model also indicates that the time required for adsorbing 50% of the initial concentration decreases with increasing flow rate and decreasing bed height. In addition to this, the estimation of time required to reach 50% breakthrough was very close to the values obtained experimentally.

The predicted breakthrough curves by the dose-response model show an excellent fit to experimental data. The column parameters associated with this model (i.e., q, b_1 and d) indicates the dependence of these parameters on flow rate and height of packed biosorbent. With the increase in mass of biosorbent from 11.71 g (10 cm) to 23.43 g (20 cm), the values of parameter q are decreased from 1.42×10^{-3} to 1.18×10^{-3} mmol g^{-1} for Pb(II). The adsorption capacity of Cd(II) at 50% break point increases from 1.15×10^{-3} to 1.82×10^{-3} mmol g^{-1} by increasing flow rate from 10 to 30 ml min^{-1} and similar effect also applies to Pb(II) sorption. The parameter b_1 associated with the volumetric throughput at 50% break point also increases with increasing bed height and flow rate. The values of q and b_1 both are in conformity with experimental data. The value of the model constant (d) increases with increase in bed height and decrease in flow rate, suggesting that parameter d of the dose-response model might be related to the design of fixed bed column with enhanced adsorption performance.

The relation between bed height and breakthrough level can be studied by applying BDST model on the column data. Figure S3 of the supplementary information shows the specific trends of BDST column parameters (i.e., N_0, K_a and Z_0) with variation of the breakthrough points. The dynamic bed capacity of Cd(II) gradually increases from 0.127 to 0.154 mmol L^{-1} in the range of 1-40% breakthrough. Within 60-95% breakthrough, the dynamic bed capacity decreases and then increases to the highest point of 0.160 mmol L^{-1}. Similar trend was observed in the sorption of Pb(II) in which there was a sharp increase in the value of N_0 from 1% to 40% breakthrough, followed by a slight increase over 60-95% breakthrough. At low breakthrough points, there exist a large number of vacant adsorption sites on the biosorbent for the metal uptake process to occur with limited or no resistive effects. The 95% breakthrough (saturation) dynamic capacity was found to be 0.160 mmol L^{-1} (0.11 mg g^{-1}) for Cd(II) and 0.198 mmol L^{-1} (0.25 mg g^{-1}) for Pb(II). Meanwhile, a gradually diminishing rate of transfer of solute from bulk fluid to the solid phase (K_a) with increasing breakthrough level was noticed and the value of parameter K_a remains relatively constant at 60-95% breakthrough. This might be ascribed to the limited extent of metal uptake because more adsorption sites were occupied and larger parts of the packed bed became saturated as the volume of effluent flowing into the column increased. The effect of diffusional resistances might also contribute significantly at high-end breakthrough levels, thus leading to a slower uptake rate of metal ions. The calculated critical bed heights at various breakthrough points show a trend similar to that of adsorption rate constant. For the breakthrough points beyond 50%, it is not possible to calculate the critical bed height due to negative value of natural logarithmic expression in Eq. (9). This argument was also confirmed by several authors[37-39], mentioning that the BDST model is used only for the interpretation of the initial part of the breakthrough curve that is up to 50% of the breakthrough.

At 50% breakthrough, the natural logarithmic expression in Eq. (8) is reduced to zero and the bed capacity was estimated to be 0.157 mmol L^{-1} (0.11 mg g^{-1}) for Cd(II) and 0.194 mmol L^{-1} (0.24 mg g^{-1}) for Pb(II). These values are considerably lower than those reported by Bhatia and his group[39] for cadmium and lead ions removal in a fixed-bed column by macro fungus. They obtained the estimated 50% breakthrough capacity per unit bed volume of 8.54 and 7.72 mmol L^{-1} for Cd(II) and Pb(II) ions, respectively. The fruit body of oyster mushroom (*Pleurotus platypus*) has been utilized for fixed-bed column removal of Cd(II) from industrial wastewater by Vimala and co-workers[40]. The breakthrough capacity per unit bed volume of 21.51 mmol L^{-1} was obtained from the BDST model prediction. Low adsorption capacity of the biomass bed was expected and it is very likely due to the initial metal concentration used in the column experiments. It is well-known that adsorption is a concentration-driven surface phenomenon and the dependence of dynamic bed capacity on the initial solute concentration is confirmed mathematically from the slope of linear BDST plot in Eq. (8). We purposely used low influent metal concentration (1.12 mg L^{-1} of Cd(II) and 2.07 mg L^{-1} of Pb(II)) to represent the actual range of heavy metals contamination in the local public water systems. Other fixed bed column parameters (e.g., linear velocity) and the characteristic of packing adsorbent might also contribute in determining the bed uptake capacity. Table 4 summarizes the comparison of adsorption performance data of various biosorbent materials for single removal of Cd(II) and Pb(II) ions in fixed bed operation. The poor prediction of the BDST model beyond 50% breakthrough point could be attributed to the complex mechanisms of metal ions binding by the biosorbent, which might involve two or more rate-limiting steps such as ion exchange, coordination, complexation, chelation, micro-precipitation, adsorption and surface adsorption-complexation. Interestingly, the curve shows an S-like pattern for the variation of critical bed height with breakthrough points (Fig. S3 of the supplementary

information), indicating the conformance between critical bed height and axial flow of MTZ inside the bed column.

Based on the analysis of all column models above, it can be deduced that the Yoon-Nelson and dose-response models give a satisfactory representation for the present column system with respect to statistical parameters (RMSE or R^2) and theoretical justification of the model parameters. From the goodness-of-fit point of view, the Thomas, Yoon-Nelson and dose-response models all are in general acceptable. While BDST model demonstrated a satisfying linear correlation between column service time and bed height, the failure of this model beyond 50% breakthrough was inevitable. Other two weaknesses of the BDST model are (1) it assumes the adsorption of single solute in the liquid-phase system and (2) it cannot address the important effects of changes in pH, ionic form of the adsorbent and solute concentration on the column performance.[37] Regarding the Thomas model, the prediction of column kinetic data was fairly well within the measured range although a quite significant deviation tends to be observed at the initial part of the breakthrough curves. Additionally, a packing height of 10 cm was considered as the optimum bed height because the increase in packing height by 5 cm and 10 cm to this point was insignificant in respect to the metal removal percentage (see Table 1).

3.4. Breakthrough modeling for biosorption of binary component metals

In this study, the simultaneous biosorption of Cd(II) and Pb(II) ions onto packed rice straw was conducted at flow rates of 10, 20 and 30 ml min^{-1} and packing heights of 10, 15 and 20 cm. An equimolar binary mixture containing 0.01 mmol L^{-1} of Cd(II) and Pb(II) ions was used as the effluent model. The breakthrough curves for binary metal solution were obtained in order to study the effect between metals and to assess the adsorption selectivity for one

metal in presence of the other in a continuous flow system. In this regard, a modified Thomas design model incorporating the sorption-inhibiting coefficients was proposed for the first time to simulate the breakthrough curves of binary metal systems. The general knowledge of binary and/or multicomponent systems is that the solute species compete with each other for the available adsorption sites on the solid surface. Such behavior would affect the rate of sorption of each solute and consequently its concentration in the adsorbed phase. Therefore, the effect of competitive adsorption should be incorporated in the design model and we introduce two dimensionless parameters as follows:

$$I_{12} = \frac{\theta_2}{\theta_1 + \theta_2} \tag{14}$$

$$I_{21} = \frac{\theta_1}{\theta_1 + \theta_2} \tag{15}$$

where θ_1 and θ_2 represent the amounts of metal ions adsorbed, I_{12} and I_{21} indicate the sorption-inhibiting coefficients of component 2 to component 1 and vice versa. θ_1 and θ_2 both treated as the fractional parameters which account for the coordination complexes of metal ions with surrounding anions on the surface at the point of saturation. Cd(II) and Pb(II) ions are designated as component 1 and component 2, respectively. By introducing parameters I_{12} and I_{21} into the original Thomas model associated to each adsorbed component, the modified Thomas model with the inclusion of competitive adsorption behavior was obtained:

$$\left(\frac{C_t}{C_0}\right)_1 = \frac{1}{1 + \exp\left[\frac{K_{\mathrm{Th},1}(1 - I_{12})}{Q}\left(q_{1,\max} m - C_{0,1} V_T\right)\right]} \tag{16}$$

$$\left(\frac{C_t}{C_0}\right)_2 = \frac{1}{1 + \exp\left[\frac{K_{\mathrm{Th},2}(1 - I_{21})}{Q}\left(q_{2,\max} m - C_{0,2} V_T\right)\right]} \tag{17}$$

where $K_{\mathrm{Th},1}$ and $K_{\mathrm{Th},2}$ are the sorption rate constants of component 1 and component 2 obtained from single solute system (L mmol^{-1} min^{-1}) while $q_{1,\max}$ and $q_{2,\max}$ are the maximum

bed sorption capacity for component 1 and component 2 in the binary system (mmol g^{-1}). Here, θ_1, θ_2, $q_{1,\,max}$ and $q_{2,\,max}$ are the fitted parameters whose values can be determined by linear or nonlinear regression methods. Several underlying assumptions of the proposed model are: (i) the adsorption equilibrium is nonlinear and can be well-represented by Langmuir isotherm; (ii) the rate driving force obeys the second-order reversible reaction kinetics, (iii) no axial dispersion and (iv) the adsorption system operates isothermally at a given condition. The solution of Eq. (16) and Eq. (17) can be easily obtained by nonlinear regression curve fitting using Systat SigmaPlot 12.3.1 software or Microsoft's Excel 'Solver' function. To start the computation, the initial values of all fitted parameters were randomly estimated with the following constraints: $\theta_1 > 0$, $\theta_2 > 0$, $q_{1,\,max} > 0$, $q_{2,\,max} > 0$ and $\theta_1 + \theta_2 < 1$. The computation lasted point after point until tolerance and convergence tests were fulfilled. We argued that total portion of metal ions adsorbed on the surface ($\theta_1 + \theta_2$) was less than unity by considering the free-volume fraction (porosity) in fixed bed where adsorption did not take place. The bed porosity (ε) can be determined by the following equation:

$$\varepsilon = 1 - \left(\rho_b / \rho_s \right) \tag{18}$$

where ρ_b and ρ_s are the tapped bulk density of packed bed (g ml^{-1}) and the density of solid particles (g ml^{-1}), which can be experimentally determined using a density meter. The applications of Eq. (16) and Eq. (17) in correlating the experimental breakthrough data for equimolar binary mixture of Cd(II) and Pb(II) ions are depicted in Figure 2 while the values of the fitted and calculated model parameters are summarized in Table 5.

It is shown in Figure 2 that the modified Thomas model can correlate the experimental breakthrough curves for binary system very well ($R^2 \sim 0.99$). The graphical fit results show that the original Thomas model (solid lines) is generally inadequate to describe the binary

adsorption breakthrough curves and an amplifying proof to this statement is indicated from the coefficient of determination ($0.5 < R^2 < 0.7$). Thus, the incorporation of the dimensionless parameters θ_1 and θ_2 accounting for the effect of competitive adsorption between two solutes is helpful to improve the goodness-of-fit of the proposed model. The values of the calculated parameters ($K_{Th,1}$ and $K_{Th,2}$) confirm the applicability of the proposed modified Thomas model in which the adsorption rate constants for each solute in the binary system are lower than the values in the single system. The presence of competing solutes not only decreases the adsorption rate constant, but also the maximum solid-phase concentration of each solute. The values of fractional parameters θ_1 and θ_2 obtained from non-linear regression analysis show that more amounts of Pb(II) are sorbed on the packed bed. Energy dispersive X-ray fluorescence (EDXRF) technique was performed to analyze the heavy metals content in the packed bed and to examine the conformity between EDXRF measurement and theoretical calculation. The results indicate an error of at most 18% between EDXRF measurement and theoretical calculation, indicating that θ_1 and θ_2 can be treated as fractional parameters to represent the amounts of solutes adsorbed in addition to empirical correction coefficients to improving the graphical fit. The maximum bed adsorption capacity of Cd(II) obtained from the prediction by modified Thomas model declines from 1.62×10^{-3} mmol g^{-1} (0.18 mg g^{-1}) to 1.41×10^{-3} mmol g^{-1} (0.16 mg g^{-1}) when Pb(II) present in the effluent for fixed bed experiment at a flow rate of 10 ml min^{-1} and 10-cm bed height. Under this condition, the maximum bed adsorption capacity of Pb(II) in the binary system was 1.57×10^{-3} mmol g^{-1} (0.33 mg g^{-1}) compared to 1.79×10^{-3} mmol g^{-1} (0.37 mg g^{-1}) in the single system. Considering the fitted parameters θ_1 and θ_2, it can be implied that Pb(II) are adsorbed more preferentially than Cd(II), which may be ascribed to smaller hydrated ionic radii of Pb(II) (4.01 Å) than Cd(II) (4.26 Å). It has been noted that the greater the ion's hydration, the farther it is from the adsorbing surface and the weaker its adsorption. A consistent link between the hydrated ionic

radii of the metals and their dynamic adsorption capacity was shown in this study. Furthermore, according to the Pearson's Hard and Soft (Lewis) Acids and Bases concept[45], Cd(II) cation belongs to the soft Lewis acids while Pb(II) cation belongs to the borderline Lewis acids. Therefore, Pb(II) cation can form strong complexes with electronegative ligands which are hard Lewis bases such as F^-, OH^- or RO^- (i.e., carboxylate oxygen) over Cd(II) cation. Increasing solution flow rate resulted in an increased amount of metal complexes on the surface while the increase in bed height gives small or no effect. Interestingly, the calculated sorption-inhibiting coefficients between two metal ions show a weak dependence on the variation in flow rate and bed height. According to the results obtained, it can be suggested that either by changing flow rate or bed height, the extent of competition between the adsorbed components is essentially unchanged. Our hypothetical conclusion is that the extent of competition between two solutes is more dependent on their initial concentrations in binary system. Accordingly, further systematic investigation in this direction is necessary to be taken by conducting the sorption-column tests using a mixture with various solute compositions.

3.5. Desorption studies and solid waste management

Once the biosorbent bed was saturated with the metal ions, it is necessary to recover the retained metal species for reusability of the bed and to reduce the incurred operating costs. The column regeneration studies were conducted for five cycles of adsorption-desorption using hydrochloric acid as the desorbing solution at three different concentrations (0.1, 0.3 and 0.5 N). The flow rate of desorbing solution was kept constant at 10 ml min^{-1} by a peristaltic pump operated in the up-flow mode. The samples from the upstream of the column were collected every 10 min for analysis. The breakthrough time (min), exhaustion time (min) and breakthrough capacity (mmol g^{-1}) were determined for each sorption-regeneration

cycle and the results are shown in Table 6. As shown in this table, a decreased breakthrough time and exhaustion time was observed as the sorption-regeneration cycles progressed. The regeneration efficiency (%) is calculated by the following equation:

$$\text{Efficiency}(\%) = q_R / q_o \times 100 \quad (20)$$

Here, q_R is the adsorption capacity of the regenerated biosorbent bed at *n*th cycle (mmol g^{-1}) and q_o is the original adsorption capacity of biosorbent bed (mmol g^{-1}). Figure 3 shows a set of graphical information about the desorption profiles of cadmium and lead ions through a 10-cm packed bed. The 93% recovery of Cd(II) was achieved by contacting the exhausted bed with 0.1 N HCl solution for 50 min, which corresponds to throughput volume of 0.50 L. A 5-fold increase in the concentration of HCl solution resulted in the enhanced desorption efficiency from 74.6% to 91.1% after 30 min elapsed. On the other hand, 0.1 N HCl (0.60 L) was used for nearly complete desorption of Pb(II) ions (~98%) and the throughput volume was reduced to 0.50 L by using 0.5 N HCl solution. Desorption of metal ions from the biosorbent wall takes place through an equivalent exchange reaction in which one mole of divalent Cd(II) or Pb(II) ions are displaced by two moles of H^+ ions.[46] Thus, an increase in the concentration of H^+ ions in the desorbing solution leads to the enhanced exchange performance between H^+ ions and metal ions at the solid-solution interfaces.

The stability performance of biosorbent bed for up to five successive sorption-regeneration cycles is evaluated and the results are presented in Figure 3B. Prior to further cycles of adsorption-desorption, the eluted bed was washed with deionized water for several times until the pH of the washing solution was in the range of 5.0-6.0. The washing step is essential to remove excess H^+ ions deposited on the biosorbent surface. It was shown that the bed adsorption capacity was nearly same for two cycles and then dropped progressively from the third cycle up to the fifth. Desorption of sorbed Pb(II) was nearly 90-92% while more than

94% of sorbed Cd(II) was desorbed in each successive cycle. Lower desorption efficiency of Pb(II) reflects once more the higher adsorption affinity of the biosorbent for this metal ion. Compared to the original bed sorption capacity, the values correspond to 84.64% for Cd(II) and 79.50% for Pb(II) after the fifth cycle, showing good adsorptive retention efficiency although the biosorbent bed had been reused for a few times. By the end of the fifth cycle, about 2.97 and 3.26 L of individual effluents containing Cd(II) or Pb(II) ions could be treated effectively to reach the permissible concentration prior to discharge. The loss of biosorption performance after the bed has been regenerated and reused consecutively was mainly due to the detrimental effects of desorbing solution.[47] The continual contact between HCl solution and biosorbent bed not only resulted in the dislocation of sorbed metal ions, but also a gradual deterioration of the biosorbent structure. SEM image in Fig. 3C shows some visible changes on the biosorbent surface structure after multiple sorption-regeneration cycles, indicating the leaching effect of acid (HCl) during desorption and may be responsible for the lessening metal biosorption capacity of the regenerated bed. Incomplete desorption of metal ions also seems to be another plausible reason for a decrease in the bed adsorption capacity during further cycles of adsorption and desorption.

Solid waste management is an environmentally-related concern which needs to be taken into account because the disposal of metal-laden adsorbent on the land can contaminate the soil and leach into the groundwater. Therefore, the conversion of waste adsorbent materials to high-value end products is of great interest for environmental sustainability. The adsorption capacity of the regenerated bed considerably vanished after the tenth cycle where less than 10% of its original adsorption capacity was retained. Elemental analysis by an EDXRF technique showed that the biosorbent bed contains 0.15 mmol g^{-1} (1.69 wt.%) of Cd(II) and 0.16 mmol g^{-1} (3.31 wt.%) of Pb(II). One of the viable approaches to transform this solid

waste is by a two-step thermal activation process at 700 °C under nitrogen-controlled atmosphere for 4 h, followed at 900 °C for 2 h under oxidizing gas (air) environment to produce high surface area activated carbons. The porous properties and structural morphology of the resultant activated carbons are given in the supplementary information Table S1 and Figure S4, respectively. The cadmium oxide- and lead oxide-impregnated carbons both are high-value products and could be further applied as a composite electrode material for electrocatalytic sensing of gaseous, inorganic and organic analytes[48], catalysis of various oxidation and reduction reactions of gases and/or liquid chemicals[49] or sorption-based water purification[50].

3.6. Scale-up treatment of real electroplating wastewater

For the scale-up experiments, the height and internal diameter of the column used were 100 and 8 cm with a scale-up ratio of 2.50-fold and 2.67-fold, respectively from laboratory-scale glass column. The detail data of scale-up experimental parameters are given in the supplementary information Table S2. Real electroplating wastewater was collected from a metal coating and plating unit located at the Surabaya Industrial Estate Rungkut, East Java. The characteristics of the wastewater include pH, total dissolved solids (TDS) and chemical oxygen demand (COD) were analyzed as per standard methods and the average concentrations of heavy metal species were measured using an atomic absorption spectrophotometer. The results are shown in the supplementary information Table S3. The pH adjustment of the wastewater was made by appropriate addition of 0.1 N HCl solution.

The BDST laboratory-scale column parameters were used for prediction of the service time of the scaled up column. The values obtained at a given flow rate (Q) and initial feed concentration (C_0) from laboratory-scale tests were used to calculate the BDST column

parameters at different Q and C_0 without further experiments according to the relation proposed by Cooney[33]:

$$\text{new slope} = \text{old slope}\left(\frac{Q_{\text{old}}}{Q_{\text{new}}}\right) \tag{21}$$

Eq. (21) was applied for addressing the change in dynamic adsorption capacity with flow rate. The intercept of BDST equation that relates to adsorption rate constant remains unchanged with flow rate thus new intercept value equals to the old one. On the other hand, the slope and y-intercept of BDST equation both are changed when initial feed concentration is changed and the new values can be calculated as follows:

$$\text{new slope} = \text{old slope}\left(\frac{C_{0,\text{old}}}{C_{0,\text{new}}}\right) \tag{22}$$

$$\text{new intercept} = \text{old intercept}\left(\frac{C_{0,\text{old}}}{C_{0,\text{new}}}\right)\times\left(\frac{\ln\left[\left(C_{0,\text{new}}/C_{\text{b}}\right)-1\right]}{\ln\left[\left(C_{0,\text{old}}/C_{\text{b}}\right)-1\right]}\right) \tag{23}$$

Figure S5a shows the breakthrough curves for individual heavy metals present in the real wastewater after biosorption through a 10-cm bed height. It can be shown that the breakthrough curves for biosorption of Cu(II), Cd(II) and Pb(II) ions evolved in the same way, resembling the typical 'S-shape' while the deformed breakthrough curves are observed for Cr(VI), Fe and Ni(II) ions. The deformed breakthrough curves for Cr(VI), Fe and Ni(II) ions might be ascribed to slow adsorption kinetics of these metal ions due to competitive adsorption effect with other metal ions that possess higher specific binding affinity for particular surfaces. The biosorbent bed also exhibited lower adsorption capacity of Cd(II) (6.84×10^{-4} mmol g^{-1}) and Pb(II) (9.64×10^{-4} mmol g^{-1}) in the case of real wastewater compared to those in single and binary synthetic effluents. The loss of adsorption capacity might be attributed to the presence of multi-metal ions in the real wastewater. Figure S5b shows the removal percentage of each heavy metal and it is obvious that more than 50% of

total Cd(II) and Pb(II) ions in the real wastewater can still be removed by a proportional amount of packed biosorbent.

The plots of the bed service time at breakthrough obtained from experimental measurements and prediction by Eqs. (22) and (23) for Cd(II) and Pb(II) ions are presented in the supplementary information Fig. S5c. For other heavy metals, the figures are not presented due to the unavailability of column data from laboratory-scale experiments. In this figure, it can be seen that for a 10-cm bed height, the predicted 1% breakthrough service time for Cd(II) and Pb(II) ions was 30 and 37 min, respectively. However, the predicted values are quite different from experimental results where the 1% breakthrough service time was 18 min for Cd(II) and 28 min for Pb(II). This might suggest that the application of BDST relation proposed by Cooney for column scale-up purposes was limited to an adsorption system under comparable circumstances. Because real electroplating wastewater was used in the scale-up experiments while synthetic aqueous solution of Cd(II) and Pb(II) ions were used in the laboratory-scale tests, it is reasonable to obtain a fairly large deviation between experimental and predicted breakthrough service time from two adsorption systems with differences in characteristics.

Conclusions

Rice straw-packed column demonstrated a potential capability to remove toxic Cd(II) and Pb(II) ions from single and binary aqueous solutions. The breakthrough and saturation of the column strongly depended on the flow rate and bed height. Longer service time of the column could be established with higher bed height and lower effluent flow rate. The Yoon-Nelson and dose-response models were successfully applied to describe the breakthrough curves for single metal systems obtained under varying bed heights and flow rates. Both empirical

models were able to provide satisfying correlation of experimental column data from the coefficient of determination (R^2) and theoretical justification of the model parameters. The binary breakthrough curves for binary metal system could be reasonably well-fitted by the modified Thomas model. The analysis of the binary breakthrough curves revealed that the extent of adsorption competition between the adsorbed solutes did not appear to be greatly affected by the variation in flow rate and bed height. The packed biomass showed good reusability during multiple sorption-regeneration cycles without showing any considerable loss in the metal sorption capacity. Investigation of the adsorption performance on real electroplating wastewater containing multiple metal ions demonstrated that the packed bed procedure can be applied in a fascinating way, provided that the pH of the wastewater was adjusted to a value between 5.5 and 6. The utilization of spent rice straw can be considered as a cheap and renewable biosorbent material for the effective and concomitantly removal of several metal ions in the large-scale wastewater treatment unit.

Acknowledgements

A grant co-financed by the International Foundation for Science (IFS), Stockholm, Sweden and the Organization for the Prohibition of Chemical Weapons (OPCW) to Felycia Edi Soetaredjo, Ph.D. is acknowledged. National Taiwan University of Science and Technology (NTUST) is gratefully acknowledged for providing SEM and EDX facility.

References

1. V. K. Gupta and I. Ali, *Sep. Purif. Technol.*, 2000, **18**, 131-140.
2. ATSDR, Priority List of Hazardous Substances, http://www.atsdr.cdc.gov/SPL/ Accessed 25 October, 2012.
3. E. Pehlivan, T. Altun and S. Parlayici, *Food Chem.*, 2012, **135**, 2229-2234.

4. I. Larraza, M. Lopez-Gonzalez, T. Corrales and G. Marcelo, *J. Colloid Interface Sci.*, 2012, **385**, 24-33.

5. J. Huang, M. Ye, Y. Qu, L. Chu, R. Chen, Q. He and D. Xu, *J. Colloid Interface Sci.*, 2012, **385**, 137-146.

6. M. Irani, M. Amjadi and M. A. Mousavian, *Chem. Eng. J.*, 2011, **178**, 317-323.

7. T. S. Anirudhan and S. S. Sreekumari, *J. Environ. Sci. (China)*, 2011, **23**, 1989-1998.

8. L. Fan, C. Luo, Z. Lv, F. Lu and H. Qiu, *Colloids and Surfaces B*, 2011, **88**, 574-581.

9. S. Chowdhury and P. D. Saha, *Colloids and Surfaces B*, 2011, **88**, 697-705.

10. X. Zhang, H. Su, T. Tan and G. Xiao, *J. Hazard. Mater.*, 2011, **193**, 1-9.

11. Y. Tian, M. Wu, X. Lin, P. Huang and Y. Huang, *J. Hazard. Mater.*, 2011, **193**, 10-16.

12. L. Huang, C. Xiao and B. Chen, *J. Hazard. Mater.*, 2011, **192**, 832-836.

13. E. S. Abdel-Halim and S. S. Al-Deyab, *Carbohydr. Polym.*, 2012, **87**, 1863-1868.

14. X. Chen, K. F. Lam, S. F. Mak and K. L. Yeung, *J. Hazard. Mater.*, 2011, **186**, 902-910.

15. T. Y. Kim, S. K. Park, S. Y. Cho, H. B. Kim, Y. Kang, S. D. Kim and S. J. Kim, *Korean J. Chem. Eng.*, 2005, **22**, 91-98.

16. V. K. C. Lee, J. F. Porter and G. McKay, *Ind. Eng. Chem. Res.*, 2000, **39**, 2427-2433.

17. H. D. Doan, A. Lohi, V. B. H. Dang and T. Dang-Vu, *Process Saf. Environ. Prot.*, 2008, **86**, 259-267.

18. I. A. Aguayo-Villarreal, A. Bonilla-Petriciolet, V. Hernandez-Montoya, M. A. Montes-Moran and H. E. Reynel-Avila, *Chem. Eng. J.*, 2011, **167**, 67-76.

19. V. J. P. Vilar, C. M. S. Botelho and R. A. R. Boaventura, *Adsorption*, 2007, **13**, 587-601.

20. S. Mohan and G. G. Sreelakshmi, *J. Hazard. Mater.*, 2008, **153**, 75-82.

21. X. Luo, Z. Deng, X. Lin and C. Zhang, *J. Hazard. Mater.*, 2011, **187**, 182-189.

22. D. C. K. Ko, J. F. Porter and G. McKay, *Chem. Eng. Sci.*, 2005, **60**, 5472-5479.

23. C. W. Cheung, C. K. Chan, J. F. Porter and G. McKay, *Environ. Sci. Technol.*, 2001, **35**, 1511-1522.

24. B. Chen, C. W. Hui and G. McKay, *Water Res.*, 2001, **35**, 3345-3356.

25. P. A. Kumar and S. Chakraborty, *J. Hazard. Mater.*, 2009, **162**, 1086-1098.

26. D. K. C. Ko, J. F. Porter and G. McKay, *Water Res.*, 2001, **35**, 3876-3886.

27. K. Nakamoto, *Infrared and Raman Spectra of Inorganic and Coordination Compounds: Part B: Applications in Coordination, Organometallic, and Bioorganic Chemistry*, Wiley Interscience, New York, 6th edn., 2008.

28. H. C. Thomas, *J. Am. Chem. Soc.*, 1944, **66**, 1664-1666.

29. Y. H. Yoon and J. H. Nelson, *Am. Ind. Hyg. Assoc. J.*, 1984, **45**, 509-516.

30. G. S. Bohart and E. Q. Adams, *J. Am. Chem. Soc.*, 1920, **42**, 523-544.

31. R. A. Hutchins, *Chem. Eng. (N.Y.)*, 1973, **80**, 133-138.

32. G. Yan, T. Viraraghavan and M. Chen, *Adsorpt. Sci. Technol.*, 2001, **19**, 25-43.

33. D. O. Cooney, *Adsorption Design for Wastewater Treatment*, CRC Press, Boca Raton, 1998.

34. H. Muhamad, H. Doan and A. Lohi, *Chem. Eng. J.*, 2010, **158**, 369-377.

35. K. Vijayaraghavan, J. Jegan, K. Palanivelu and M. Velan, *Chemosphere*, 2005, **60**, 419-426.

36. G. Yan and T. Viraraghavan, *Bioresour. Technol.*, 2001, **78**, 243-249.

37. V. Sarin, T. S. Singh and K. K. Pant, *Bioresour. Technol.*, 2006, **97**, 1986-1993.

38. J. Cruz-Olivares, C. Perez-Alonso, C. Barrera-Diaz, F. Urena-Nunez, M. C. Chaparro-Mercado and B. Bilyeu, *Chem. Eng. J.*, 2013, **228**, 21-27.

39 M. Jain, V.K. Garg and K. Kadirvelu, *Bioresour. Technol.*, 2013, **129**, 242-248.

40. Z. Zulfadhly, M. D. Mashitah and S. Bhatia, *Environ. Pollut.*, 2001, **112**, 463-470.

41. R. Vimala, D. Charumathi and N. Das, *Desalination*, 2011, **275**, 291-296.

42. A. Singh, D. Kumar and J. P. Gaur, *Water Res.*, 2012, **46**, 779-788.

43. Y. Long, D. Lei, J. Ni, Z. Ren, C. Chen and H. Xu, *Bioresour. Technol.*, 2014, **152**, 457-463.

44. A. S. A. Aziz, L. A. Manaf, H. C. Man and N. S. Kumar, *Environ. Sci. Pollut. Res.*, 2014, **21**, 7996-8005.

45. R. G. Pearson, *J. Am. Chem. Soc.*, 1963, **85**, 3533-3539.

46. I. A. H. Schneider, J. Rubio and R. W. Smith, *Int. J. Miner. Process.*, 2001, **62**, 111-120.

47. B. Volesky, J. Weber and J. M. Park, *Water Res.*, 2003, **37**, 297-306.

48. B. Sljukic, C. E. Banks, A. Crossley and R. G. Compton, *Anal. Chim. Acta*, 2007, **587**, 240-246.

49. K. Otto, C. Lehman, L. Bartosiewicz and M. Shelef, *Carbon*, 1982, **20**, 243-251.

50. M. R. Yu, Y. Y. Chang and J. K. Yang, *Environ. Technol.*, 2012, **33**, 1553-1559.

Table 1 The breakthrough parameters for single biosorption of Cd(II) and Pb(II) ions at various bed heights and flow rates

Metal	Bed Height (cm)	Flow Rate (ml min^{-1})	t_b (min)†	t_e (min)†	MTZ (cm)$^{\zeta}$	q_b ($\times 10^{-4}$ mmol g^{-1})‡	V_e (ml)	% R¶
Cadmium	10	10	68	292	7.67	5.81	2920	93.5
		20	27	210	8.71	4.61	4200	85.6
		30	15	205	9.27	3.84	6150	78.7
	15	10	109	361	10.47	6.20	3610	93.8
		20	48	240	12.00	5.46	4800	85.8
		30	25	233	13.39	4.27	6990	79.2
	20	10	158	393	11.96	6.74	3930	94.0
		20	67	272	15.07	5.72	5440	86.1
		30	35	267	17.38	4.48	8010	79.4
Lead	10	10	72	270	7.33	6.15	2700	95.4
		20	32	212	8.49	5.47	4240	87.6
		30	18	178	8.99	4.61	5340	81.2
	15	10	118	361	10.10	6.72	3610	95.7
		20	51	271	12.18	5.81	5420	87.8
		30	29	210	12.93	4.95	6300	81.5
	20	10	171	395	11.34	7.30	3950	96.1
		20	73	300	15.13	6.23	6000	88.2
		30	42	237	16.46	5.38	7110	82.0

† Experimentally determined from Fig. (1), t_b and t_e were considered at 1% and 95% break points, respectively

‡ The bed adsorption capacity at 1% breakthrough, determined by Eq. (3)

$^{\zeta}$ Mass transfer zone is calculated by $Z = (1 - t_b / t_e)$ where Z is the bed height (cm)

¶ Removal percentage was calculated by dividing M_r with the influent metal load ($V_e \bullet C_0$)

Table 2 The correlation parameters of the Thomas, Yoon-Nelson and dose-response models for single removal of Cd(II) and Pb(II) ions at varying bed heights (solution flow rate: 10 ml min^{-1} and influent metal concentration: 0.01 mmol L^{-1})

Thomas Model						
Metal	Bed Height (cm)	K_{Th} (L $mmol^{-1}$ min^{-1})	q_{max} (mmol g^{-1})	q_{bed} (mmol g^{-1})†	RMSE	R^2
Cadmium	10	3.06	1.62×10^{-3}	1.39×10^{-3}	0.056	0.948
	15	2.71	1.39×10^{-3}	1.18×10^{-3}	0.046	0.976
	20	2.64	1.20×10^{-3}	1.09×10^{-3}	0.029	0.981
Lead	10	3.25	1.79×10^{-3}	1.53×10^{-3}	0.089	0.940
	15	2.87	1.54×10^{-3}	1.29×10^{-3}	0.025	0.972
	20	2.79	1.32×10^{-3}	1.18×10^{-3}	0.016	0.984
Yoon-Nelson Model		K_{YN} (min^{-1})	τ (min)	τ_{exp} (min)	RMSE	R^2
Cadmium	10	0.030	194	182	0.060	0.943
	15	0.027	246	236	0.048	0.967
	20	0.026	285	293	0.034	0.982
Lead	10	0.034	170	180	0.079	0.949
	15	0.028	241	238	0.051	0.960
	20	0.026	282	271	0.023	0.977
Dose-Response Model		q (mmol g^{-1})	b_1 (ml)	d	RMSE	R^2
Cadmium	10	1.47×10^{-3}	1721.37	3.94	0.038	0.993
	15	1.30×10^{-3}	2284.10	4.86	0.031	0.995
	20	1.15×10^{-3}	2694.45	6.42	0.021	0.998
Lead	10	1.42×10^{-3}	1428.62	3.89	0.025	0.997
	15	1.27×10^{-3}	2231.39	4.89	0.024	0.996
	20	1.18×10^{-3}	2764.74	6.44	0.022	0.997

† Dynamic uptake capacity, determined by Eq. (1)

Table 3 The correlation parameters of the Thomas, Yoon-Nelson and dose-response models for single removal of Cd(II) and Pb(II) ions at varying solution flow rates (bed height: 20 cm and influent metal concentration: 0.01 mmol L^{-1})

Thomas Model						
Metal	Flow Rate (ml min^{-1})	K_{Th} (L $mmol^{-1}$ min^{-1})	q_{max} (mmol g^{-1})	q_{bed} (mmol g^{-1})†	RMSE	R^2
Cadmium	10	2.64	1.20×10^{-3}	1.09×10^{-3}	0.029	0.981
	20	3.15	1.03×10^{-3}	0.85×10^{-3}	0.022	0.958
	30	3.36	0.92×10^{-3}	0.79×10^{-3}	0.052	0.965
Lead	10	2.79	1.32×10^{-3}	1.18×10^{-3}	0.016	0.984
	20	3.24	1.22×10^{-3}	1.08×10^{-3}	0.024	0.941
	30	3.45	1.11×10^{-3}	0.96×10^{-3}	0.023	0.958
Yoon-Nelson Model		K_{YN} (min^{-1})	τ (min)	τ_{exp} (min)	RMSE	R^2
Cadmium	10	0.026	285	293	0.034	0.982
	20	0.029	168	147	0.074	0.954
	30	0.033	157	142	0.041	0.968
Lead	10	0.026	282	271	0.023	0.977
	20	0.030	190	180	0.051	0.948
	30	0.035	139	128	0.051	0.939
Dose-Response Model		q (mmol g^{-1})	b_1 (ml)	d	RMSE	R^2
Cadmium	10	1.15×10^{-3}	2694.45	6.42	0.021	0.998
	20	1.21×10^{-3}	2835.03	3.89	0.022	0.998
	30	1.82×10^{-3}	4264.26	3.64	0.032	0.995
Lead	10	1.18×10^{-3}	2764.74	6.44	0.022	0.997
	20	1.46×10^{-3}	3420.78	4.03	0.030	0.995
	30	1.57×10^{-3}	3678.51	3.62	0.023	0.998

† Dynamic uptake capacity, determined by Eq. (1)

Table 4 Comparison of BDST model-predicted bed capacity of various biomass materials for the removal of Cd(II) and Pb(II) ions in fixed bed column operation

Biomass	Influent Concentration (mmol L^{-1})	Column Parameters		Predicted Bed Capacity (mmol L^{-1})	Reference
		Flow Rate (ml min^{-1})	Bed Height (cm)		
P-doped rice husk	0.05 – Pb(II)	20	10-30	2.51×10^{-3}	(20)
Wheat straw	0.89 – Cd(II)	1000	50-200	2.77	(34)
Allspice residue	0.07 – Pb(II)	20	15	11.75 – Pb(II)	(38)
Sunflower waste carbon calcium-alginate beads	0.09 – Cd(II)	1	10-30	0.07	(39)
Macro fungus (*Pycnoporus sanguineus*)	0.7 – Cd(II) 0.38 – Pb(II)	10	4-15	7.72 – Pb(II) 8.54 – Cd (II)	(40)
Macro fungus (*Pleurotus platypus*)	0.09 – Cd(II)	5	5-15	21.51	(41)
Filamentous green algae (*Spirogyra neglecta*)	0.24 – Pb(II)	5	1	0.88	(42)
Spent *Agaricus bisporus*	0.24 – Pb(II)	5	4	32.01	(43)
Palm oil boiler mill fly ash	0.18 – Cd(II)	5	1-2	75.80	(44)
Rice straw	0.01 – Cd(II) 0.01 – Pb(II)	10	10-20	0.157 – Cd(II) 0.194 – Pb(II)	This study

Table 5 The fitted and calculated parameters of the modified Thomas model for binary sorption of Cd(II) and Pb(II) ions at various bed heights and flow rates

Bed Height (cm)	Flow Rate (ml min^{-1})	Experimental		Fitted Parameters				Calculated Parameters				RMSE	R^2
		$q_{bed,1}$ (mmol g^{-1})	$q_{bed,2}$ (mmol g^{-1})	θ_1	θ_2	$q_{max,1/bin}$ (mmol g^{-1})	$q_{max,2/bin}$ (mmol g^{-1})	I_{12}	I_{21}	$K_{Th,1/bin}$ (L mmol^{-1} min^{-1})	$K_{Th,2/bin}$ (L mmol^{-1} min^{-1})		
10	10	1.24×10^{-3}	1.44×10^{-3}	0.35	0.42	1.41×10^{-3}	1.57×10^{-3}	0.55	0.45	1.38	1.79	0.024	0.987
	20	1.74×10^{-3}	1.96×10^{-3}	0.37	0.43	1.96×10^{-3}	2.13×10^{-3}	0.54	0.46	1.69	1.92	0.017	0.993
	30	2.06×10^{-3}	2.38×10^{-3}	0.40	0.45	2.33×10^{-3}	2.69×10^{-3}	0.53	0.47	1.86	2.08	0.019	0.995
15	10	0.95×10^{-3}	1.12×10^{-3}	0.36	0.42	1.08×10^{-3}	1.29×10^{-3}	0.54	0.46	1.25	1.55	0.021	0.989
	20	1.31×10^{-3}	1.53×10^{-3}	0.38	0.44	1.46×10^{-3}	1.75×10^{-3}	0.54	0.46	1.57	1.84	0.017	0.992
	30	1.49×10^{-3}	1.75×10^{-3}	0.40	0.45	1.62×10^{-3}	1.92×10^{-3}	0.53	0.47	1.74	1.94	0.017	0.995
20	10	8.74×10^{-4}	9.48×10^{-4}	0.36	0.42	9.71×10^{-4}	1.08×10^{-3}	0.54	0.46	1.21	1.51	0.020	0.984
	20	1.12×10^{-3}	1.34×10^{-3}	0.38	0.44	1.24×10^{-3}	1.44×10^{-3}	0.54	0.46	1.45	1.75	0.014	0.997
	30	1.35×10^{-3}	1.56×10^{-3}	0.41	0.46	1.48×10^{-3}	1.71×10^{-3}	0.53	0.47	1.58	1.83	0.022	0.991

Table 6 The breakthrough parameters of the original and regenerated biosorbent bed after five sorption-regeneration cycles

Metal	Cycle No.	t_b (min)	t_e (min)	q_b (mg g^{-1})†	q_e (mg g^{-1})†	Desorption (mg g^{-1})	Regeneration Efficiency (%)
Cadmium	1	68	292	0.065	0.280	0.265	Original
	2	65	287	0.062	0.276	0.263	98.57
	3	60	275	0.058	0.264	0.251	94.29
	4	54	262	0.052	0.252	0.242	90.00
	5	50	247	0.048	0.237	0.227	84.64
Lead	1	72	270	0.127	0.478	0.439	Original
	2	70	262	0.124	0.464	0.420	97.07
	3	65	252	0.115	0.446	0.411	93.31
	4	62	240	0.110	0.425	0.389	88.91
	5	57	215	0.101	0.380	0.343	79.50

Note – bed height: 10 cm and flow rate of the metal influent and desorbing solution (0.5 N HCl): 10 ml min^{-1}

† The bed adsorption capacity at 1% and 95% breakthrough refers to and respectively, calculated by Eq. (3)

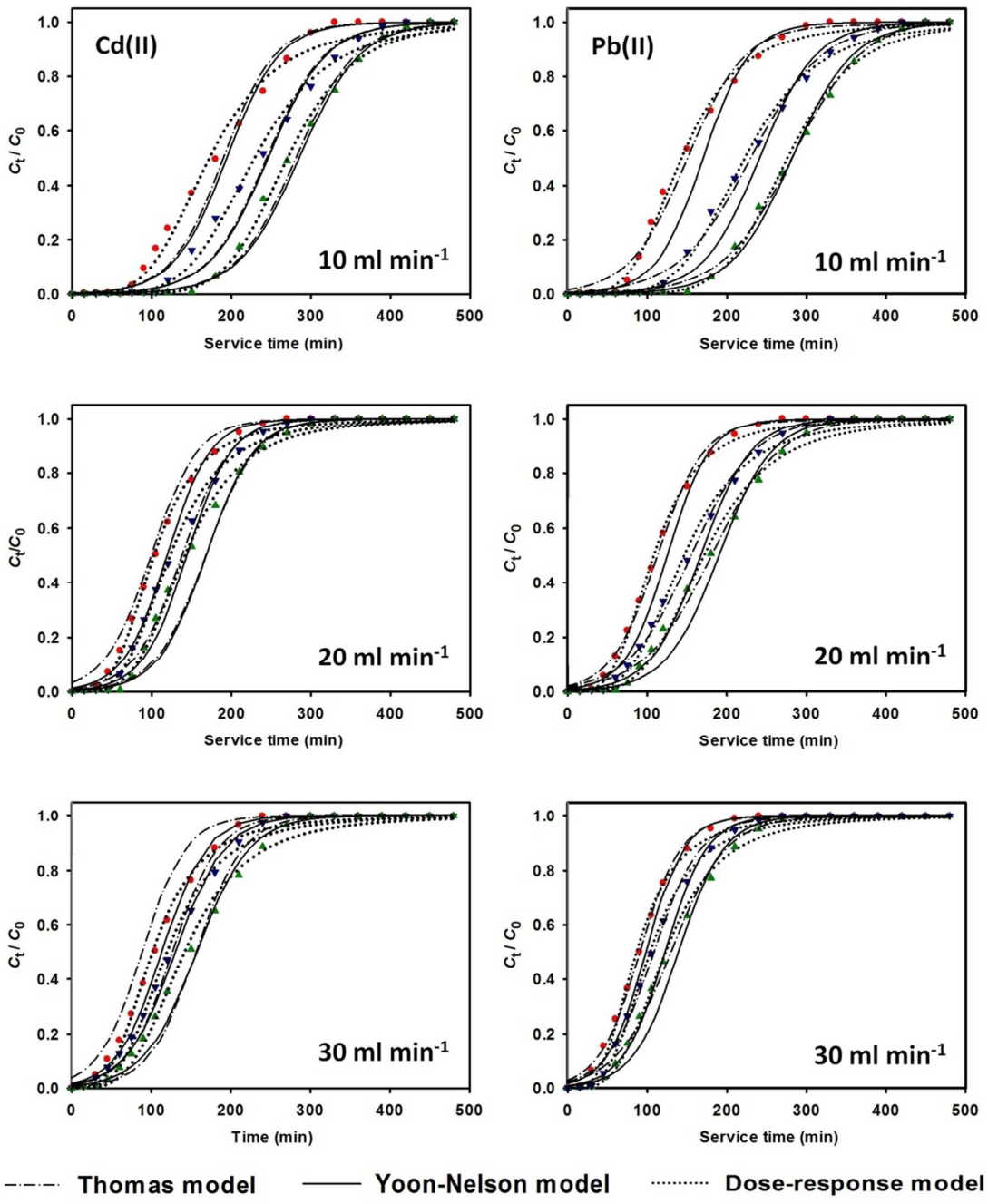

Fig. 1 Experimental breakthrough curves for single biosorption of Cd(II) and Pb(II) ions at various flow rates and bed heights (● 10 cm – ▼ 15 cm – ▲ 20 cm) and the prediction results by the Thomas, Yoon-Nelson and dose-response models

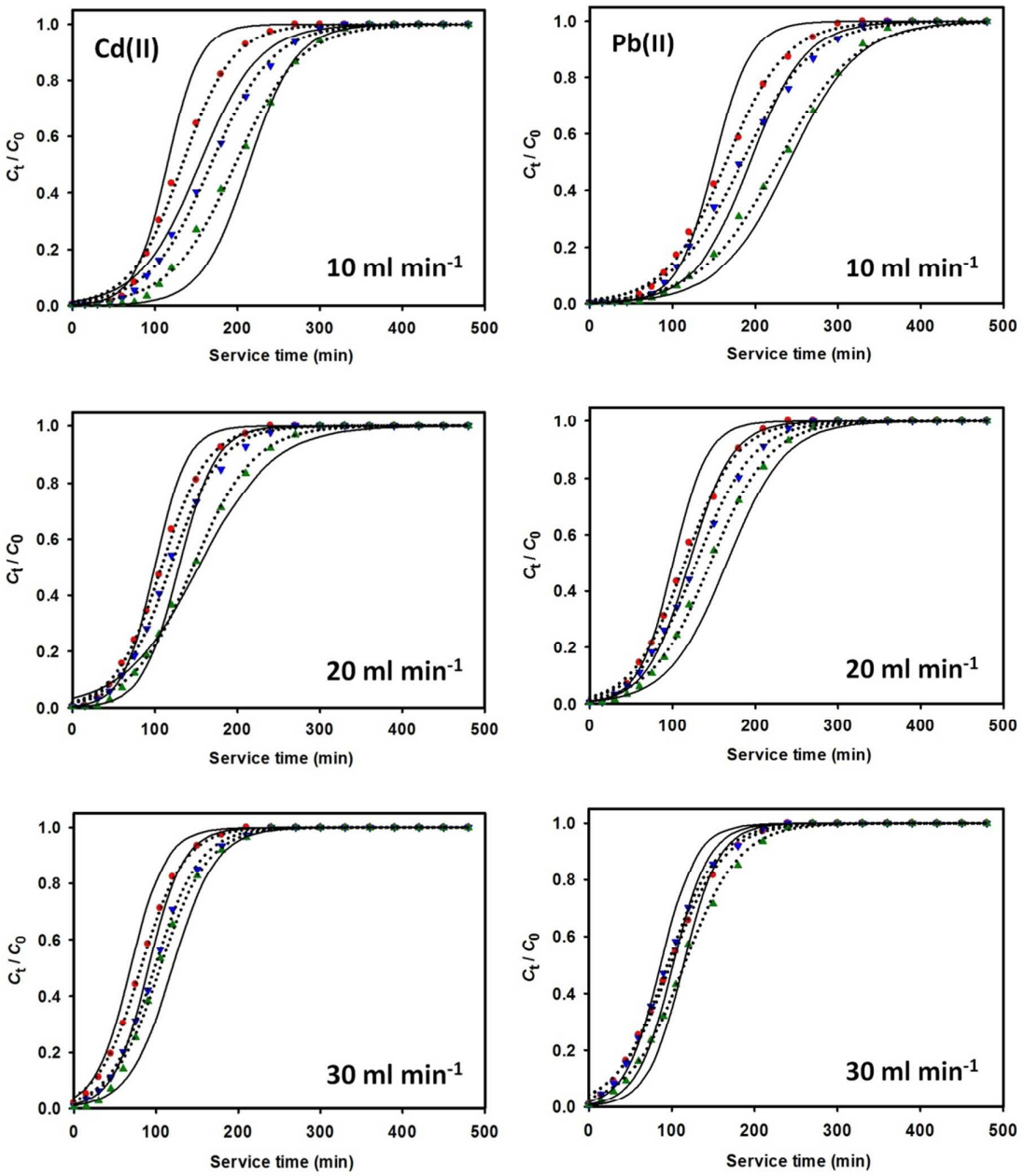

Fig. 2 Performance comparison between the original (solid lines) and modified Thomas model (dotted lines) in correlating the breakthrough curves for binary sorption of Cd(II) and Pb(II) ions at various flow rates and bed heights (● 10 cm – ▼ 15 cm – ▲ 20 cm)

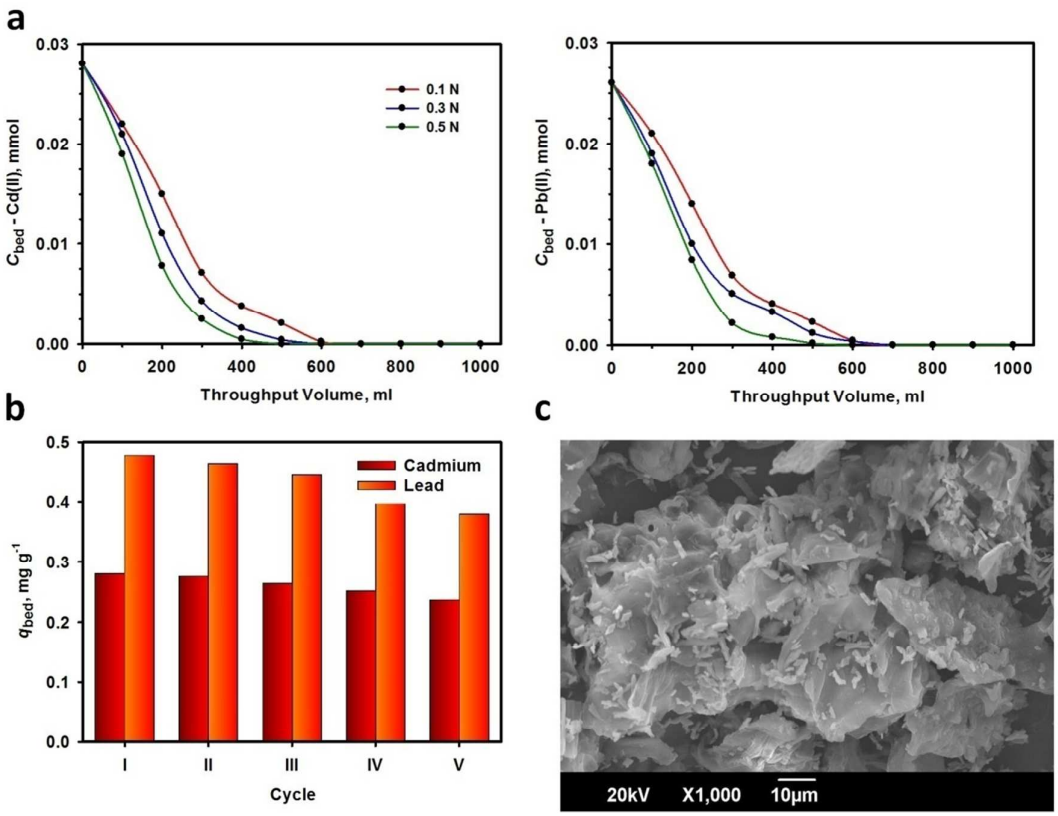

Fig. 3 Desorption curves of Cd(II) and Pb(II) ions by HCl treatment at various concentrations (a) and the metal adsorptive retention after five sorption-regeneration cycles (b); SEM image shows the resulting morphology of biosorbent after desorption with 0.5 N HCl solution (c)